Regenerative Therapy 9 (2018) 1–9

Contents lists available at ScienceDirect

Regenerative Therapy

journal homepage: http://www.elsevier.com/locate/reth

Original Article

Preparation of iPS cell-derived CD31$^+$ endothelial cells using three-dimensional suspension culture

Shinako Masuda [a], Katsuhisa Matsuura [a, b, *], Tatsuya Shimizu [a]

[a] Institute of Advanced Biomedical Engineering and Science, Tokyo Women's Medical University, 8-1 Kawada-cho, Shinjuku, Tokyo 162-8666, Japan
[b] Department of Cardiology, Tokyo Women's Medical University, 8-1 Kawada-cho, Shinjuku, Tokyo 162-8666, Japan

ARTICLE INFO

Article history:
Received 9 January 2018
Received in revised form
24 May 2018
Accepted 22 June 2018

Keywords:
Human inducible pluripotent stem cells
Three-dimensional suspension culture
Endothelial cell differentiation
Microvascular network formation

ABSTRACT

A well-organised vascular network is essential for metabolic exchange to maintain homoeostasis in the body. Therefore, for progress in regenerative medicine, it is particularly important to establish methods of vascularization in bioengineered three-dimensional (3D) functional tissues. In addition, it is necessary to develop methods to supply a large number of iPS cell-derived endothelial cells for fabricating the vascular network structure. There are already many reports on the method of inducing the differentiation of endothelial cells from iPS cells using 2D culture. However, there are few reports on methods for preparing a large number of iPS cell-derived endothelial cells. Therefore, we developed methods for inducing vascular endothelial cells from human inducible pluripotent stem (hiPS) cells using 3D suspension culture. hiPS cell-derived CD31$^+$ cells expressed several endothelial marker genes and formed endothelial cell network structures, similar to human umbilical vein endothelial cells. These results indicate that hiPS cell-derived CD31$^+$ cells may be a useful cell source for pre-vascularised network structures in 3D functional tissues, and it is important to develop 3D mass culture system for preparing a large number of cells to fabricate bioengineered tissues.

1. Introduction

It is anticipated that the application of three-dimensional (3D) bioengineered tissues in the fields of regenerative medicine and drug screening will become possible. The limitation of perfusion from the medium into 3D tissue is about 100–200 μm, although this depends on the type of tissue [1]. In addition to oxygen exchange, vascular network structures play essential roles in the supply of nutrition and the removal of metabolic waste products. Therefore, it is essential to establish methods for fabricating vascular structures within 3D tissues. We previously developed cell sheet engineering to create functional 3D tissues by layering two-dimensional confluent cell sheets harvested from temperature-responsive culture surfaces [2–5]. In the transplantation of layered neonatal rat cardiac cell sheets, CD31$^+$ cells within the graft formed a pre-vascular network, resulting in the connection between transplanted graft and host tissue and therefore to better engraftment [6,7]. We also established novel 3D tissue models with a perfusable vascular structure using *ex vivo* or *in vitro* vascular beds [8,9]. Because of the incomplete vascular structures within the abovementioned 3D tissue models, the establishment of fully vascularised host-connectable tissue is considered to be one of the major challenges for future work. An important factor in this context is human umbilical vein endothelial cells (HUVECs), which are currently used as vascular cells when reconstructing various tissues. However, to reconstruct the tissues more accurately, it is considered necessary to perform tissue-specific optimisation of the type of blood vessels, such as arterial or venous, and the vessel diameter.

Pluripotent stem cells are a promising cell source for fabricating bioengineered 3D tissues because of their potential to differentiate into various types of cells and their ability to supply a large number of cells. We previously reported on large-scale bioreactor systems for cardiovascular differentiation from mouse embryonic stem (ES) cells and human inducible pluripotent stem (hiPS) cells, as well as the fabrication of cardiac cell sheets from these pluripotent stem cell-derived cardiovascular cells [10–12]. It has been reported that pluripotent stem cell-derived cardiac tissues prepared by co-

* Corresponding author. Institute of Advanced Biomedical Engineering and Science, Tokyo Women's Medical University, 8-1 Kawada-cho, Shinjuku, Tokyo 162-8666, Japan. Fax: +81 3 3359 6046.
E-mail address: matsuura.katsuhisa@twmu.ac.jp (K. Matsuura).
Peer review under responsibility of the Japanese Society for Regenerative Medicine.

https://doi.org/10.1016/j.reth.2018.06.004

culture of vascular cells enhance the performance of transplanted grafts [13,14]. Building on previous work with the aim of providing a large number of endothelial cells for fabricating 3D-functional vascularised tissues, we here developed methods for inducing $CD31^+$ cells from hiPS cells using a bioreactor system, demonstrated pre-vascular network formation of hiPS cell-derived $CD31^+$ cells by co-culture with normal human dermal fibroblasts (NHDFs) and compared their characteristic features with those of tissue-derived endothelial cells.

2. Methods

2.1. Antibodies

Monoclonal antibodies for human kinase-insert domain receptor (KDR) conjugated with phycoerythrin (R&D Systems, Minneapolis, MN, USA) and monoclonal antibodies for human CD31 conjugated with phycoerythrin (R&D Systems) were used for magnetic-activated cell sorting (MACS) separation. Phycoerythrin-conjugated monoclonal antibodies for human vascular endothelial (VE)-cadherin (R&D Systems) and monoclonal antibodies for human CD31 conjugated with phycoerythrin were used for immunocytochemistry. Fluorescein-conjugated monoclonal antibody for murine human CD31 (R&D Systems) was used as the primary antibody for immunocytochemistry.

2.2. Cell culture

NHDFs and HUVECs were purchased from Lonza (Walkersville, MD) and maintained in accordance with the manufacturer's instructions. Human iPS (hiPS) cells (253G1) were purchased from RIKEN (Tsukuba, Japan) and maintained in Primate ES Cell Medium (ReproCELL Inc., Tokyo, Japan), supplemented with 5 ng/mL basic fibroblast growth factor (ReproCELL) on mitomycin C-treated mouse embryonic fibroblasts. Cells were passaged as small clumps every 3 days using CTK solution (ReproCELL).

2.3. Preparation of $CD31^+$ cells

$CD31^+$ cells were prepared from differentiated hiPS cells (253G1). A single-use bioreactor and a magnetic stirrer were purchased from ABLE Corporation & Biott Corporation (Tokyo, Japan). To induce differentiation, small colonies of hiPS cells were seeded into culture vessels (approximately 2×10^5 cells/mL mTeSR1 containing Y27632 [10 μM]) and cultured until day 2. From day 2 to day 7, embryoid bodies (EBs) were cultured in StemPro34 containing 50 μg/mL ascorbic acid (Sigma–Aldrich, St. Louis, MO), 2 mM L-glutamine (Life Technologies, Carlsbad, CA) and 400 μM 1-thioglycerol (Sigma–Aldrich). On day 2, medium was supplemented with 12 ng/mL BMP4, 5 ng/mL bFGF and 6 ng/mL Activin A (R&D Systems) and removed them at day 5. On day 5, medium was supplemented with 10 ng/mL vascular endothelial growth factor (VEGF) (R&D Systems) and 10 ng/mL bFGF and removed them at day 7. On day 7, EBs were enzymatically dissociated and subjected to MACS (Miltenyi Biotec GmbH, Germany) to separate KDR^+ cells. KDR^+ cells were re-cultured with 10 ng/mL VEGF and 10 ng/mL bFGF onto ColIV-coated tissue culture dishes. Three days after the re-culture, induced $CD31^+$ cells were isolated from re-cultured KDR^+ cells by MACS.

2.4. Immunocytochemistry

Cells were fixed with 5% dimethyl sulfoxide in methanol and blocked with 1% skimmed milk. The fixed cells were then stained with primary antibody overnight at 4 °C, followed by incubation with secondary antibody for 3 h at 4 °C. Nuclei were visualised with Hoechst 33342.

2.5. Image acquisition and data analysis

Images of $CD31^+$ cells were collected using an ImageXpress Ultra confocal high-content screening system (Molecular Devices, LLC, Sunnyvale, CA, USA). The number of $CD31^+$ cells, tube length and branch point of the $CD31^+$ cell network structure were assessed using MetaXpress software (Molecular Devices, LLC) [15].

2.6. Quantitative real-time polymerase chain reaction

First-strand cDNA was synthesised using a High Capacity cDNA Reverse Transcription Kit (ABI) from purified total RNA isolated using an RNeasy Plus Mini Kit (Qiagen, Hilden, Germany). First-strand synthesis was performed on a T3000 ThermoCycler (Biometra). Quantitative real-time PCR was carried out using a StepOnePlus system (ABI), in accordance with the manufacturer's instructions. The expression levels of genes for cadherin 5 (CDH5), KDR, platelet/endothelial adhesion molecule 1 (Pecam1) and von Willebrand factor (vWF) were analysed by TaqMan gene expression assay (ABI) and gene expression was normalised to endogenous β-actin.

2.7. RNA extraction and microarray analysis

Total RNA of human umbilical artery endothelial cells (HUAECs) was purchased from Toyobo (Osaka, Japan). Total RNA of HUVECs and hiPS cell-derived $CD31^+$ cells was extracted from cells using an RNeasy Plus Mini Kit (Qiagen), in accordance with the manufacturer's instructions. RNA quantity and quality were determined using a Nanodrop ND-1000 spectrophotometer (Thermo Fisher Scientific Inc.) and an Agilent Bioanalyzer (Agilent Technologies, Santa Clara, CA), as recommended. Total RNA was amplified and labelled with Cyanine 3 (Cy3) using Agilent Low Input Quick Amp Labeling Kit, one-colour (Agilent Technologies), following the manufacturer's instructions. For each hybridisation, 0.60 μg of Cy3-labelled cRNA was fragmented and hybridised at 65 °C for 17 h to an Agilent SurePrint G3 Human GE v3 8 × 60K Microarray (Design ID: 072363). Intensity values of each scanned feature were quantified using Agilent feature extraction software version 11.5.1.1, which performs background subtractions. We only used features that were flagged as no errors (detected flags) and excluded features that were not positive, not significant, not uniform, not above background, that were saturated and population outliers (not detected and compromised flags). Normalisation was performed using Agilent GeneSpring software version 14.8 (per chip: normalisation to 75th percentile shift). There are a total of 50,599 probes on the Agilent SurePrint G3 Human GE v3 8 × 60K Microarray (Design ID: 072363) without control probes.

2.8. Integrated bioinformatic analysis of differentially-expressed genes

Gene Ontology annotation of the differentially-expressed genes within the main category of biological process was performed using the Database for Annotation, Visualization and Integrated Discovery (DAVID 6.8; https://david.ncifcrf.gov). A three-way Venn diagram was also constructed using VENNY 2.1 (http://bioinfogp.cnb.csic.es/tools/venny/).

2.9. Statistical analysis

Data are presented as means ± standard deviations. Student's *t*-tests or paired *t*-tests were used to analyse differences between two

groups, as appropriate. The statistical significance of differences between groups was calculated by one-way analysis of variance. Differences were considered significant when $p < 0.05$.

3. Results

3.1. Differentiation and characterisation of CD31$^+$ cells from human iPS cells

Reports have indicated that human pluripotent stem cells were induced to differentiate into cardiovascular cells via the intermediate of mesodermal precursor cells in 2D culture [16–20]. To achieve the successful induction of differentiation in 2D culture, supplementation with growth factors or low molecular weight compounds at appropriate times is beneficial. It is also necessary to scale up the differentiation culture in order to prepare a sufficiently large number of target cells for successful tissue preparation and cell transplantation, but it is difficult to simply scale up a differentiation induction system in 2D culture. To overcome this problem, in recent years, we have reported the mass culture of undifferentiated human iPS cells and large-scale culture for myocardial differentiation induction using 3D suspended stirring culture [12]. Here, we attempted the mass preparation of vascular endothelial cells using 3D suspension culture. For the induction of differentiation, hiPS cells were cultured in a bioreactor with 30-mL vessels (Fig. 1). Following treatment with CTK solution, small colonies of hiPS cells were seeded into 30-mL culture vessels. When comparing the gene expression of common endothelial markers such as cadherin 5 (CDH5), KDR and CD31 at various time points until day 7, their expression levels were significantly higher after day 7 of differentiation compared with those of undifferentiated states (Fig. 2A, upper). Then, cell aggregates on day 7 were dissociated and subjected to MACS to isolate cardiovascular progenitor KDR$^+$ cells. When KDR$^+$ and KDR$^-$ cells were plated onto ColIV-coated tissue culture dishes with VEGF and bFGF for 3 days, the cells derived from KDR$^+$ cells were 70%–80% positive for CD31, while the cells induced from the KDR$^-$ cell fraction were approximately 10% positive for CD31 (Fig. 2B). When CD31$^+$ cells were isolated from KDR$^+$ cell-derived cells by MACS and cultured on ColIV-coated dishes for 3 days, a typical cobblestone structure appeared (Fig. 2C). These cells also formed sprouted branch-like structures when placed on top of Matrigel (Fig. 2D). After 3 days of re-culture, the expression of several endothelial marker genes was assessed among hiPS cell-derived CD31$^+$ cells, HUVECs and HUAECs by real-time reverse transcription polymerase chain reaction (RT-PCR) (Fig. 2E). The expression of the cadherin 5, PECAM1 and vWF genes in hiPS cell-derived CD31$^+$ cells was similar to that in tissue-derived endothelial cells. Although the gene expression of KDR was higher than that of tissue-derived endothelial cells, this might have been due to the response to the high concentration of VEGF in the differentiation medium. Moreover, these CD31$^+$ cells were found to be positive for CD31 (98.4% ± 2.0%) and vascular endothelial cadherin (99.1% ± 0.5%) at cell–cell junctions, as observed in other endothelial cells (Fig. 2F). These findings suggest that KDR$^+$ cells differentiated in 3D suspension culture further differentiated into endothelial cells.

Although 3D suspension culture using a 30-mL vessel successfully induced KDR$^+$ cells and subsequent CD31$^+$ endothelial cells, the number of isolated KDR$^+$ and CD31$^+$ cells was $1.0 \times 10^6 \pm 1.0 \times 10^5$ cells (Fig. 3A upper) and $5.1 \times 10^5 \pm 0.5 \times 10^5$ cells (Fig. 3C upper), respectively. Next we attempted to collect more number of endothelial cells in a single run using larger vessels (100-mL vessels). Studies in human pluripotent stem cells have reported that oxygen concentration influences endothelial differentiation [21,22], and we reported that 40% of saturated O_2 is the most efficient concentration for inducing differentiation into cardiomyocytes using a bioreactor [11]. Therefore, we elucidated the appropriate oxygen concentration (24% of saturated O_2 (24% O_2), 40% of saturated O_2 (40% O_2) and uncontrolled [atmospheric condition, AC]) for the induction of KDR$^+$ cells in a 100-mL vessel and compared the number of isolated KDR$^+$ cells with that in the 30-mL vessel. The number of isolated KDR$^+$ cells was almost similar among each

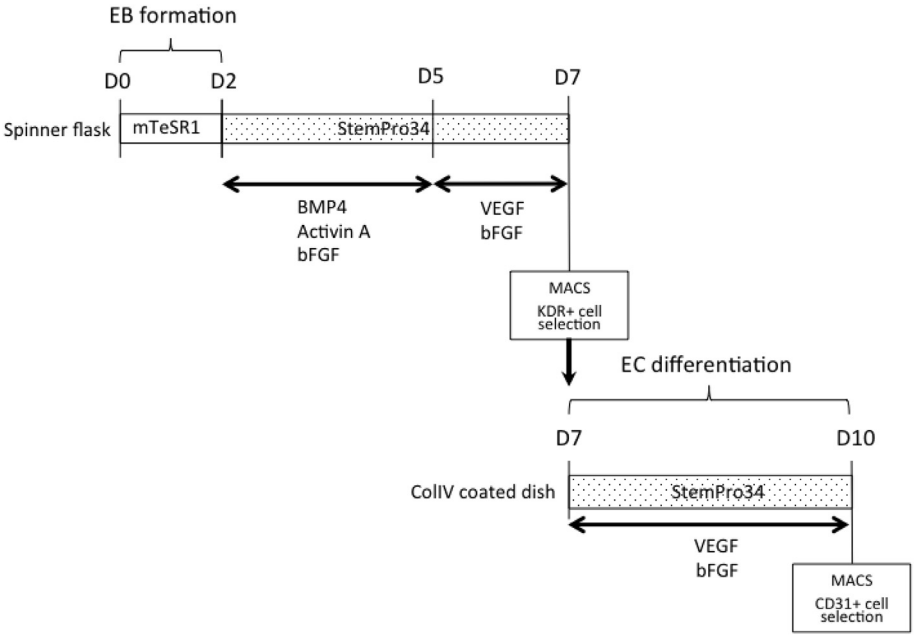

Fig. 1. Scheme of the induction of endothelial differentiation from human iPS cells in a bioreactor system. Small colonies of hiPS cells were seeded into culture vessels and incubated in mTeSR1 until day 2. From days 2–7, EBs were cultured in StemPro34 supplemented with growth factors and small molecules, as indicated by the diagram. Embryoid bodies were dissociated enzymatically and subjected to MACS to separate KDR$^+$ cells on day 7. KDR$^+$ cells were plated onto collagen IV-coated tissue culture dishes and cultured in the presence of VEGF and basic FGF for further differentiation. After 3 days of re-culture, CD31$^+$ cells were isolated from re-cultured KDR$^+$ cells by MACS.

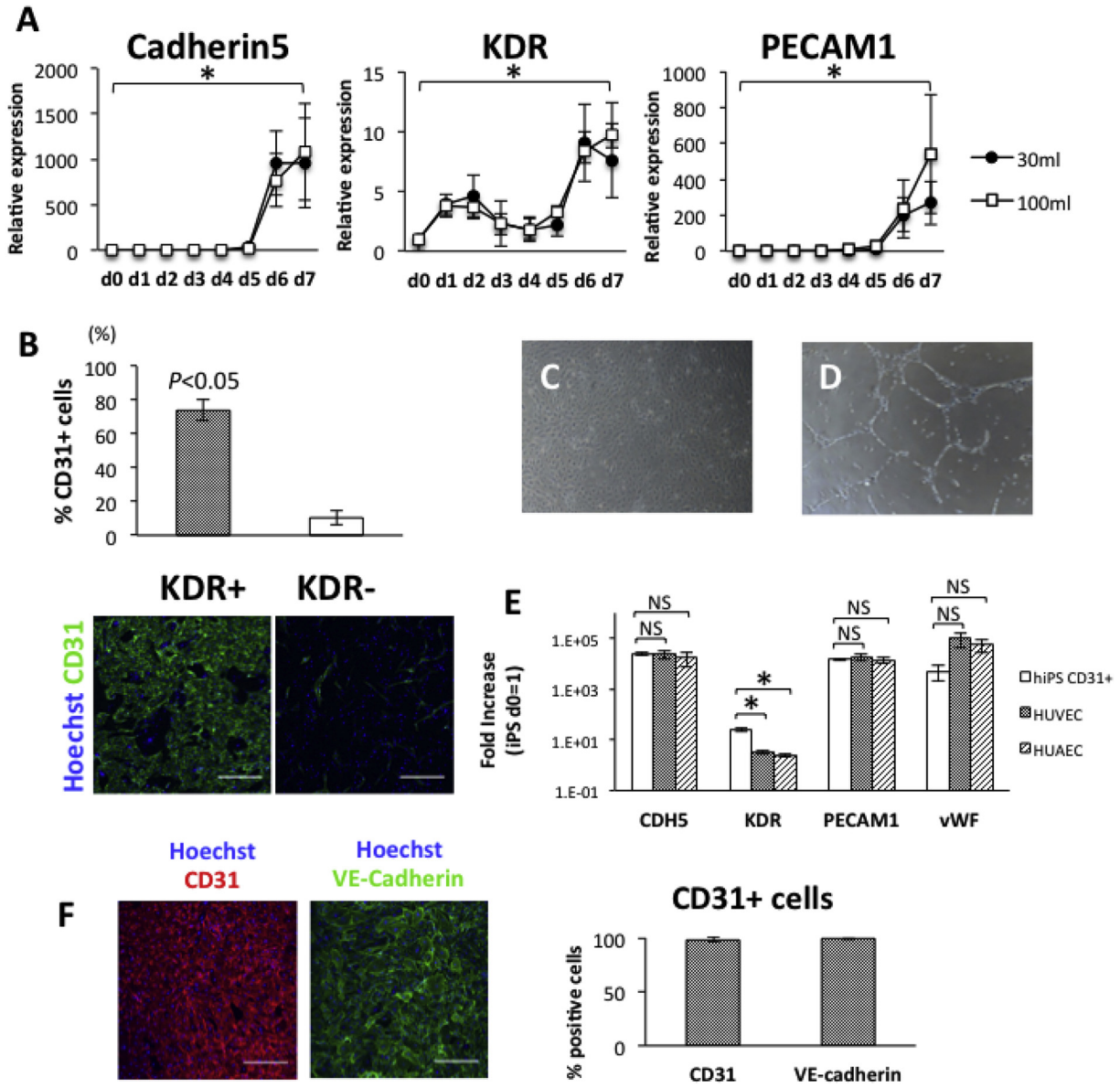

Fig. 2. Characterisation of hiPS cell-derived CD31$^+$ cells. (A) Endothelial marker gene expression in differentiated hiPS cells. hiPS cell differentiation was performed in 30- or 100-ml culture vessels. (B) Mean percentage of cells expressing CD31 on day 9 of differentiation from KDR$^+$ or KDR$^-$ cells. After 7 days of differentiation, both KDR$^+$ and KDR$^-$ cells were isolated by MACS, re-cultured onto collagen IV-coated tissue culture dishes, and immunostained with CD31 antibodies. Scale bars = 400 pm. CD31$^+$ cell number was analysed using MetaXpress software. (C) Phase-contrast image of hiPS cell-derived CD31$^+$ cells. Magnification, ×40. (D) Network formation by induced CD31$^+$ cells after 24 h of culture on top of Matrigel. Magnification, ×40. (E) Comparison of endothelial marker gene expression between hiPS cell-derived CD31$^+$ cells and tissue-derived vascular endothelial cells. The expression levels of genes were analysed by Taqman gene expression assay and gene expression was normalised to endogenous β-actin. (F) Immunostaining of CD31$^+$ cells derived from hiPS cells on day 13 of differentiation. CD31 (left panel, red) and vascular endothelial cadherin (right panel, green). (B-F) hiPS cell differentiation from day 0 to day 7 was performed in 30-ml culture vessels. Nuclei were stained with Hoechst 33342 (blue) in (B) and (F). Scale bars = 400 pm in (B) and (F). Values are shown as mean ± standard deviation for at least three separate experiments in (A), (B), (E) and (F). Asterisk indicates statistically significant difference ($p < 0.05$). NS, not significant.

oxygen concentration (24% O_2: 3.8 × 10^6 ± 1.7 × 10^6 cells, 40% O_2: 3.1 × 10^6 ± 1.2 × 10^6 cells, AC: 2.8 × 10^6 ± 1.5 × 10^6 cells) and that was approximately 3 times the number of isolated KDR$^+$ cells in the 30-mL vessel (9.6 × 10^5 ± 1.0 × 10^5 cells, Fig. 3A upper). The proportion of KDR$^+$ cells to the initial iPS cell number (24% O_2: 18.8% ± 8.3%, 40% O_2: 15.3% ± 6.1%, AC: 14.2% ± 7.5%, 30 mL: 16.6% ± 1.6%, Fig. 3B) and to the total cell number on day 7 (24% O_2: 3.6% ± 1.0%, 40% O_2: 4.1% ± 2.3%, AC: 3.4% ± 1.9%, 30 mL: 2.2% ± 0.2%, Fig. 3A lower) was also similar among the three conditions and in the 30-mL vessel. Next we induced CD31$^+$ endothelial cells from KDR+ cells isolated from each oxygen concentration condition. The number of isolated CD31$^+$ cells was almost similar among each condition (24% O_2: 3.1 × 10^6 ± 1.2 × 10^6 cells, 40% O_2: 1.9 × 10^6 ± 1.2 × 10^6 cells, AC: 2.1 × 10^6 ± 1.4 × 10^6 cells) and that was about 4 times the number of isolated CD31$^+$ cells in the 30-mL vessel (5.1 × 10^5 ± 0.5 × 10^5 cells, Fig. 3C upper). The proportion of CD31$^+$ cells to the initial iPS cells (24% O_2: 15.5% ± 6.1%, 40% O_2: 9.6% ± 5.9%, AC: 10.5% ± 6.9%, 30 mL: 8.5% ± 0.9%, Fig. 3D) and to the total cell number on day 10 (24% O_2: 53.0% ± 12.5%, 40% O_2: 48.7% ± 23.9%, AC: 43.7% ± 22.1%, 30 mL: 54.4% ± 34.1%, Fig. 3C lower) was similar among three conditions in the 100-mL vessel and 30-mL vessel. Consistent with the yield of KDR$^+$ cells, gene expression of common endothelial cells markers in 100-mL vessels (40% of saturate O_2) was remarkably upregulated after day 6 of differentiation and the expression levels were similar between the 100-mL and 30-mL vessel (Fig. 2A). These findings suggest that the

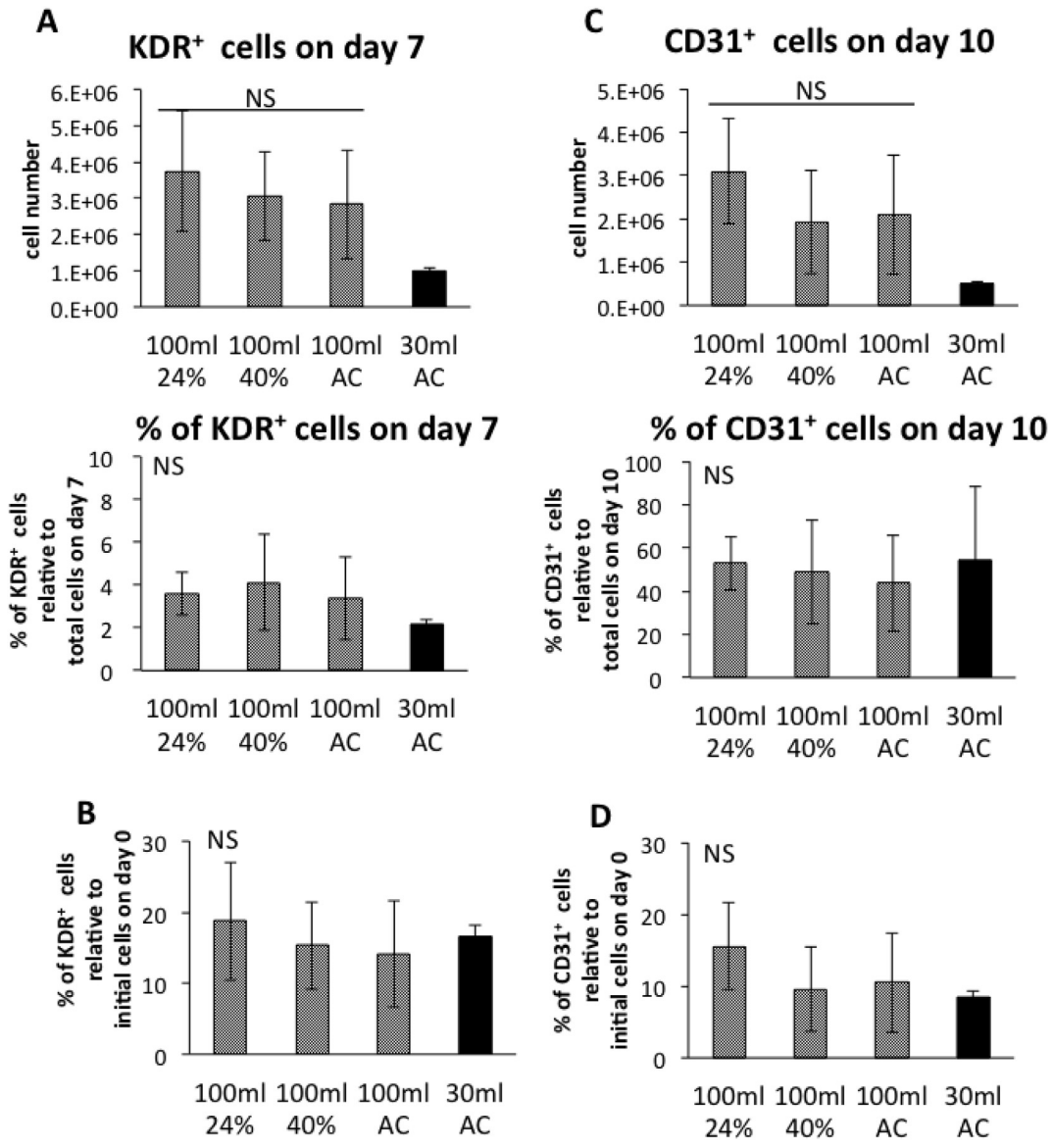

Fig. 3. Comparison of cell expansion and differentiation efficiency of hiPS cells in a bioreactor. hiPS cell differentiation was performed in 30- or 100-ml culture vessels with various dissolved oxygen conditions. AC, uncontrolled (atmospheric condition). (A) The number of isolated KDR$^+$ cells on day 7 (upper) and the total cell number on day 7 (lower). (B) Percentage of isolated KDR$^+$ cells on day 7 was calculated by comparing the initial cell number on day 0. (C) The number of isolated CD31$^+$ cells on day 10 (upper) and the total cell number on day 10 (lower). (D) Percentage of isolated CD31$^+$ cells on day 10 was calculated by comparing the initial cell number on day 0. Values are shown as mean ± standard deviation for three separate experiments. NS, not significant.

number of endothelial cells induced when using larger vessels is similar to that using smaller ones, and cultivation in larger vessel may be useful for collecting more endothelial cells in a single run.

3.2. iPS cell-derived CD31$^+$ cells form vascular network structures in co-culture

In agreement with the behaviour of HUVECs, hiPS cell-derived CD31$^+$ cells formed a sprouted branch-like structure on the Matrigel (Fig. 2D). To examine whether CD31$^+$ cells derived from hiPS cells form a network structure in co-culture, hiPS cell-derived CD31$^+$ cells and NHDFs were mixed at a ratio of 1:4 and cultured in Dulbecco's Modified Eagle's medium supplemented with 10% foetal bovine serum at 3×10^5 cells/cm^2. At 4 days, the formation of the network structure was observed in co-culture with hiPS cell-derived CD31$^+$ cells (Fig. 4A). When images of the CD31$^+$ cell network structure in co-cultured cells were collected using a confocal high-content screening system and several parameters of the CD31$^+$ cell network structure were calculated using MetaXpress software (Fig. 4B), the value of total tube length and the total number of branch points from hiPS cell-derived CD31$^+$ cell co-culture were not significantly different to those from HUVEC co-culture. Despite the ability to form vascular network structures in co-culture, the proliferation of hiPS cell-derived CD31$^+$ cells in 2D culture was considerably lower than that of HUVECs (Fig. 4C).

3.3. Comparison of gene expression among hiPS cell-derived CD31$^+$ cells and tissue-derived endothelial cells

To clarify the difference of the proliferative ability between hiPS cell-derived CD31$^+$ cells and HUVEC, gene expression was assessed using microarrays among three samples from each of the hiPS cell-derived CD31$^+$ cells, HUVECs and HUAECs, as a control of tissue-

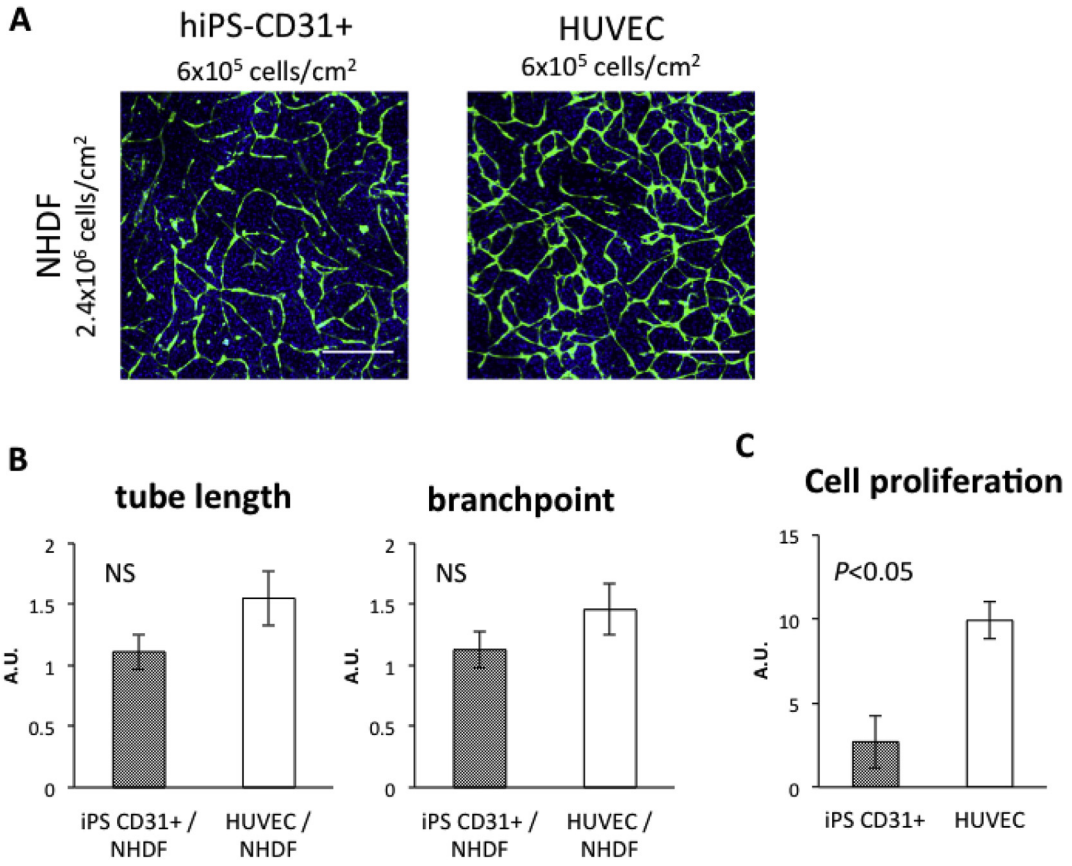

Fig. 4. Pre-vascular network structure formed in co-culture. (A) Either hiPS cell-derived CD31$^+$ cells or HUVECs were co-cultured with NHDFs. Images of the CD31$^+$ cell network structure were collected by ImageXpress Ultra confocal high-content screening system (Molecular Devices) and analysed by MetaXpress software (Molecular Devices). Scale bars = 400 μm. (B) The software scored total tube length and branch point of the CD31$^+$ cell network structure. (C) Comparison of cell proliferation between hiPS cell-derived CD31$^+$ cells and HUVECs. Growth rate was calculated by comparing the total cell number on day 0 with that on day 3. Values are shown as mean ± standard deviation for three separate experiments. Values are shown as mean ± standard deviation for five separate experiments. NS, not significant.

derived endothelial cells. The microarray data were first analysed by principal component analysis in order to assess the similarity between the samples (Fig. 5A). Principal component analysis classified them for each group of hiPS cell-derived CD31$^+$ cells, HUVECs and HUAECs. Greater than twofold differences in expression were observed in 3088 and 6195 genes between HUVECs and HUAECs, and between hiPS cell-derived CD31$^+$ cells and HUAECs, respectively, while only 1229 genes were identified to be more than twofold differentially expressed between hiPS cell-derived CD31$^+$ cells and HUVECs, suggesting a similarity in the gene expression between hiPS cell-derived CD31$^+$ cells and HUVECs. To assess the similarity among them, we used the Database for Annotation, Visualization and Integrated Discovery (DAVID 6.8) [23,24] online resource for gene annotation and functional enrichment analysis of differentially expressed genes (fold change > 2). There were 134, 209, and 125 Gene Ontology (GO) terms within the main category of the biological process in hiPS cell-derived CD31$^+$ cells vs. HUVECs, hiPS cell-derived CD31$^+$ cells vs. HUAECs, and HUVECs vs. HUAECs, respectively. A Venn diagram was constructed to show the overlap of GO terms (Fig. 5B, upper). This was based on the calculated p-values for the main category of biological process in the comparisons of hiPS cell-derived CD31$^+$ cells vs. HUVECs, hiPS cell-derived CD31$^+$ cells vs. HUAECs, and HUVECs vs. HUAECs. A total of 8 GO terms were common to the hiPS cell-derived CD31$^+$ cells vs. HUVECs and HUVEC vs. HUAECs. Of these, 5 GO terms were also common to the hiPS cell-derived CD31$^+$ cells vs. HUAECs, while the remaining three were defined as a common set of GO terms between hiPS cell-derived CD31$^+$ cells and HUAECs relative to HUVECs. In contrast, there were 28 and 29 common sets of GO terms between hiPS cell-derived CD31$^+$ cells and HUVECs relative to HUAECs, and between HUVECs and HUAECs relative to hiPS cell-derived CD31$^+$ cells, respectively, suggesting the similarity of the biological processes between hiPS cell-derived CD31$^+$ cells and HUVECs, and between HUVECs and HUAECs. Furthermore, Venn diagrams prepared using GO terms based on biological processes extracted separately for genes whose expression was upregulated or downregulated (fold change > 2 or fold change < −2) suggested the similarities between hiPS cell-derived CD31$^+$ cells and HUVECs, and between HUVECs and HUAECs in both cases (Fig. 5B, lower, left and right). Despite the similarity in gene expression, the proliferation of hiPS cell-derived CD31$^+$ cells was considerably lower than that of HUVECs (Fig. 4C). To clarify the reason for of this difference, GO terms based on biological processes were extracted from groups of genes whose expression was upregulated or downregulated in hiPS cell-derived CD31$^+$ cells relative to HUVECs, and the top 20 GO terms are shown in descending order of *p*-value (Figs. S1 and S2 and Table S1). Subsets from the upregulated genes were found to be involved in 'negative regulation of ERK1 and ERK2 cascade', 'Wnt signalling pathway, calcium modulating pathway', and 'negative regulation of phosphatidylinositol 3-kinase signalling', and a subset from the downregulated genes was found to be involved in 'oxidation—reduction process', suggesting that cell proliferation might be negatively regulated in hiPS cell-derived CD31$^+$ cells. In addition, subsets from the upregulated genes were found to be involved

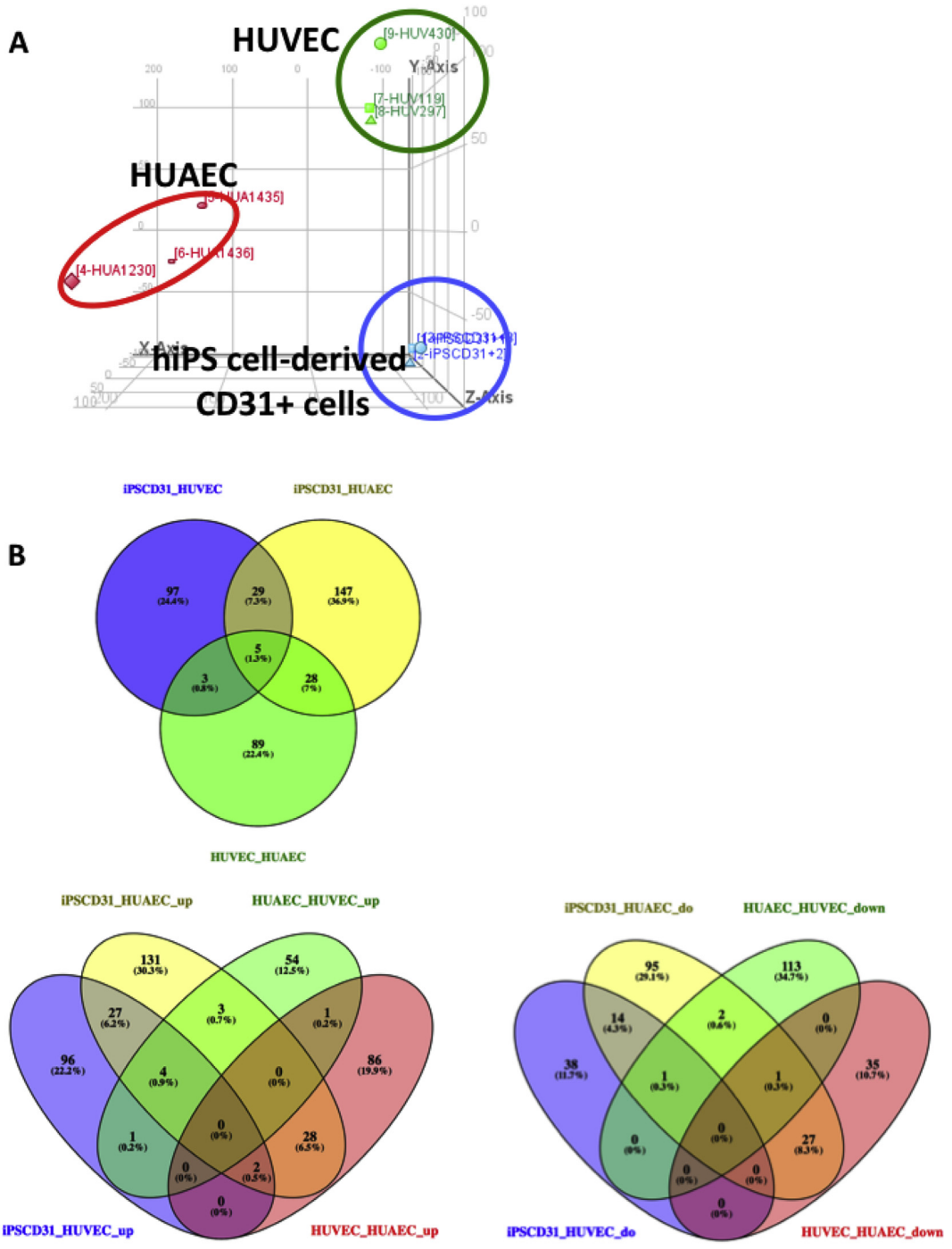

Fig. 5. (A) Principal component analysis of microarray data among hiPS cell-derived CD31$^+$ cells, HUVECs and HUAECs. (B) Venn diagram showing overlapping GO terms of biological process among hiPS cell- derived CD31$^+$ cells vs. HUVECs, hiPS cell-derived CD31$^+$ cells vs. HUAECs and HUVECs vs. HUAECs. Three-way Venn diagram showing the numbers of common and specific GO terms (upper), four-way Venn diagram showing the numbers of common and specific upregulated (lower, left) and downregulated (lower, right) GO terms. (C) Gene ontology classification of upregulated and downregulated genes in hiPS cell- derived CD31$^+$ cells relative to HUVECs with respect to biological process. Gene ontology biological process terms were derived using the DAVID bioinformatics database. 'Count' is the number of genes associated with the GO term and '*p*-value' represents the significance of the GO term.

in 'cell adhesion', 'positive regulation of GTPase activity' and 'regulation of Rho protein signal transduction', and subsets from the downregulated genes were found to be involved in 'cell-substrate junction assembly' and 'endothelial cell migration', suggesting that the difference in the abilities of the cells to undergo adhesion and migration might be involved in the lower proliferation of hiPS cell-derived CD31$^+$ cells.

4. Discussion

For the successful formation of a microvascular structure when fabricating 3D tissues, the supply of a large number of endothelial cells is important. iPS cells are considered a promising cell source for regenerative medicine and for the fabrication of 3D-tissue models in order to supply a large number of cells. The successful

induction of mesodermal progenitor cells and cardiovascular cells from hiPS cells in 2D culture using OP9 co-culture and EB formation or directed differentiation methods have been reported [16–20]. Moreover, we reported a 3D-suspension culture for the induction of cardiovascular progenitor fetal liver kinase-1-positive cells from mouse ES cells for the fabrication of bioengineered pre-vascularised cardiac cell sheets [15]. We present here the induction of cardiovascular progenitor KDR$^+$ cells and CD31$^+$ endothelial cells from hiPS cells using bioreactor systems. Sequential supplementation for differentiation to KDR$^+$ cells and CD31$^+$ cells were performed in a manner almost similar to protocol by White et al. [20], KDR$^+$ cells were induced with BMP4, Activin A and bFGF from day 2 to day 5, and with VEGF and bFGF from day 5 to day 7. CD31$^+$ cells were differentiated from KDR$^+$ cells for 3 days induction supplemented with VEGF and bFGF. White et al. reported that the percentage of KDR$^{high/med}$ varied widely between cell lines and between differentiations even in the same cell line with a range of 6.8%–73%. In our differentiation process, approximately 2.2–4.1% of the total cell number on day 7 was isolated as KDR$^+$ cells between 30- and 100-mL cultures, it may depend on the difference of cell lines. In addition, EC were induced from KDR$^{high/med}$ cell population in greater than 90%, while induced in fewer than 10% from KDR$^{med/low}$ cell population [20]. We report here 70%–80% of KDR$^+$ cells became positive for CD31 while the cells induced from the KDR$^-$ cell fraction were approximately 10% positive for CD31. Finally, the yield of CD31$^+$ cells is 8.5–15.5% between 30- and 100-mL cultures, and the yield from protocol by White et al. varied among batches and lines (15–40%) [20]. These results suggested that cardiovascular progenitor and endothelial cells were differentiated in our bioreactor system. Although the yield of EC remains insufficient in our system, adaptation of chemically defined medium and novel marker for cardiovascular progenitor cells [19] may help to improve the efficiency of our differentiation system. Moreover, endothelial lineage was highly induced from hiPS cells by sequential switching of defined ECMs [25], therefore, the yield of EC may be improved by supplement with optimized ECM-derived fragment in bioreactor system. In an attempt to scale up the culture volume for KDR$^+$ cell induction, the cell density on day 7 was at the same level in 30- and 100-mL cultures (data not shown). In terms of the differentiation efficiency of KDR$^+$ cells, there was no significant difference between the two 30- and 100-mL cultures. These results indicate that our bioreactor systems could be scaled up without any reduction of efficiency of differentiation of KDR$^+$ cells, and could provide elemental technology for the development of an automatic system for iPS cell differentiation.

Gene expression analysis revealed that CD31$^+$ cells induced from hiPS cells were also positive for several endothelial markers. Upon comparing the gene expression of common endothelial markers, cadherin 5, KDR, CD31 and vWF, their expression in hiPS cell-derived CD31$^+$ cells was similar to that in other tissue-derived endothelial cells, suggesting that the hiPS cell-derived CD31$^+$ cells were endothelial cells.

Co-culture study revealed that hiPS cell-derived CD31$^+$ cells have the ability to form a vascular network structure. In the co-culture with NHDFs, either hiPS cell-derived CD31$^+$ cells or HUVECs formed pre-vascular network structures in accordance with the increment of the cell number of NHDFs (data not shown). It has been reported that fibroblasts play key roles in promoting angiogenesis through the secretion of growth factors and the production of extracellular matrix molecules [26–28]. Moreover, sprouting was also induced in the co-culture with other primary endothelial cells, namely both HAECs and human cardiac microvascular endothelial cells (HMVEC-Cs), in a manner dependent on the number of NHDF cells (data not shown). These results suggest the supportive effect of NHDFs on the sprouting of endothelial cells.

Recently, it has been reported that the tissue microenvironment plays crucial roles in the acquisition of tissue-specific properties by endothelial cells [29]. HUVECs are committed cells derived from the umbilical cord, while iPS cell-derived CD31$^+$ cells are considered to be uncommitted because of the fact that they are not exposed to an environment that can induce mature endothelial cell specification. Moreover, hiPS cells were differentiated into endothelial cells and maturated to brain microvascular endothelial-like cells by co-culture with C6 glioma cells, although HUVECs might not be converted in the same culture conditions [30]. These observations suggest that cell character and behaviour are affected by the level of cell maturity and factors in the environment.

In Fig. 4C, we presented that the proliferation of hiPS cell-derived CD31$^+$ cells was considerably lower than that of HUVEC; therefore, we performed the comparison of gene expression in Fig. 5 to clarify the difference of the proliferative activity between hiPS cell-derived CD31$^+$ cells and HUVECs. Principal component analysis suggested a similarity in gene expression between hiPS cell-derived CD31$^+$ cells and HUVECs, but when GO terms based on biological processes were extracted from groups of genes whose expression was upregulated or downregulated in hiPS cell-derived CD31$^+$ cells relative to HUVECs, it suggested that several signal cascades related to cell proliferation, adhesion and migration were involved in the lower proliferation of hiPS cell-derived CD31$^+$ cells. We consider the development of a culturing method that enables long-term amplification of iPS cell-derived CD31$^+$ cells as a future subject.

We present here the differentiation induction of iPS cell-derived CD31$^+$ cells using 3D suspension culture and the evaluation of the properties of iPS cell-derived CD31$^+$ cells using 253G1 line. We understand that it is difficult to generalize the results obtained in one line, and this is the limitation of this study, but we confirmed the differentiation of iPS cell-derived CD31$^+$ cells from 201B7 line using the same method (data not shown). In the future, standardization of differentiation induction method using plural strains and development of proliferation method of iPS cell-derived endothelial cells are required.

Pre-vascular network formation is important for the fabrication of 3D bioengineered tissue *in vitro*. To prepare the large number of hiPS cell-derived CD31$^+$ cells needed for 3D tissue construction, it is necessary to improve the efficiency with which the cells differentiate and proliferate after the induction of differentiation. Since the expression of endothelial marker genes and the ability to perform cell sprouting in hiPS cell-derived endothelial cells are equivalent to those of tissue-derived endothelial cells, it is suggested that improving proliferative ability is a key factor for preparing a large number of hiPS cell-derived endothelial cells in the future.

Conflict of interest

Tatsuya Shimizu is a member of the scientific advisory board and a stakeholder of CellSeed Inc. Tokyo Women's Medical University receives a research fund from CellSeed Inc. Tatsuya Shimizu and Katsuhisa Matsuura are inventors of bioreactor systems.

Acknowledgements

This work was funded by a grant from Projects for Technological Development in Research Center Network for Realization of Regenerative Medicine of the Japan Science and Technology Agency, JST and Japan Agency for Medical Research and Development, AMED under Grant Number JP17bm0404015.

Appendix A. Supplementary data

Supplementary data related to this article can be found at https://doi.org/10.1016/j.reth.2018.06.004.

References

[1] Colton CK. Implantable biohybrid artificial organs. Cell Transplant 1995;4:415–36.
[2] Okano T, Yamada N, Sakai H, Sakurai Y. A novel recovery system for cultured cells using plasma-treated polystyrene dishes grafted with poly(N-isopropylacrylamide). J Biomed Mater Res 1993;27:1243–51.
[3] Okano T, Yamada N, Okuhara M, Sakai H, Sakurai Y. Mechanism of cell detachment from temperature-modulated, hydrophilic-hydrophobic polymer surfaces. Biomaterials 1995;16:297–303.
[4] Haraguchi Y, Shimizu T, Sasagawa T, Sekine H, Sakaguchi K, Kikuchi T, et al. Fabrication of functional three-dimensional tissues by stacking cell sheets in vitro. Nat Protoc 2012;7:850–8.
[5] Masuda S, Shimizu T. Three-dimensional cardiac tissue fabrication based on cell sheet technology. Adv Drug Deliv Rev 2016;96:103–9.
[6] Sekiya S, Shimizu T, Yamato M, Kikuchi A, Okano T. Bioengineered cardiac cell sheet grafts have intrinsic angiogenic potential. Biochem Biophys Res Commun 2006;341:573–82.
[7] Sekine H, Shimizu T, Hobo K, Sekiya S, Yang J, Yamato M, et al. Endothelial cell coculture within tissue-engineered cardiomyocyte sheets enhances neovascularization and improves cardiac function of ischemic hearts. Circulation 2008;118:S145–52.
[8] Sekine H, Shimizu T, Sakaguchi K, Dobashi I, Wada M, Yamato M, et al. In vitro fabrication of functional three-dimensional tissues with perfusable blood vessels. Nat Commun 2013;4:1399.
[9] Sakaguchi K, Shimizu T, Horaguchi S, Sekine H, Yamato M, Umezu M, et al. In vitro engineering of vascularized tissue surrogates. Sci Rep 2013;3:1316.
[10] Matsuura K, Masuda S, Haraguchi Y, Yasuda N, Shimizu T, Hagiwara N, et al. Creation of mouse embryonic stem cell-derived cardiac cell sheets. Biomaterials 2011;32:7355–62.
[11] Matsuura K, Wada M, Konishi K, Sato M, Iwamoto U, Sato Y, et al. Fabrication of mouse embryonic stem cell-derived layered cardiac cell sheets using a bioreactor culture system. PLoS One 2012;7:e52176.
[12] Matsuura K, Wada M, Shimizu T, Haraguchi Y, Sato F, Sugiyama K, et al. Creation of human cardiac cell sheets using pluripotent stem cells. Biochem Biophys Res Commun 2012;425:321–7.
[13] Masumoto H, Matsuo T, Yamamizu K, Uosaki H, Narazaki G, Katayama S, et al. Pluripotent stem cell-engineered cell sheets reassembled with defined cardiovascular populations ameliorate reduction in infarct heart function through cardiomyocyte-mediated neovascularization. Stem cells 2012;30:1196–205.
[14] Masumoto H, Ikuno T, Takeda M, Fukushima H, Marui A, Katayama S, et al. Human iPS cell-engineered cardiac tissue sheets with cardiomyocytes and vascular cells for cardiac regeneration. Sci Rep 2014;4:6716.
[15] Masuda S, Matsuura K, Mie A, Iwamiya T, Shimizu T, Okano T. Formation of vascular network structures within cardiac cell sheets from mouse embryonic stem cells. Regen Ther 2015;2:6–16.
[16] Sone M, Itoh H, Yamahara K, Yamashita JK, Yurugi-Kobayashi T, Nonoguchi A, et al. Pathway for differentiation of human embryonic stem cells to vascular cell components and their potential for vascular regeneration. Arterioscler Thromb Vasc Biol 2007;27:2127–34.
[17] Yang L, Soonpaa MH, Adler ED, Roepke TK, Kattman SJ, Kennedy M, et al. Human cardiovascular progenitor cells develop from a KDR+ embryonic-stem-cell-derived population. Nature 2008;453:524–8.
[18] James D, Nam HS, Seandel M, Nolan D, Janovitz T, Tomishima M, et al. Expansion and maintenance of human embryonic stem cell-derived endothelial cells by TGFbeta inhibition is Id1 dependent. Nat Biotechnol 2010;28:161–6.
[19] Prasain N, Lee MR, Vemula S, Meador JL, Yoshimoto M, Ferkowicz MJ, et al. Differentiation of human pluripotent stem cells to cells similar to cord-blood endothelial colony-forming cells. Nat Biotechnol 2014;32:1151–7.
[20] White MP, Rufaihah AJ, Liu L, Ghebremariam YT, Ivey KN, Cooke JP, et al. Limited gene expression variation in human embryonic stem cell and induced pluripotent stem cell-derived endothelial cells. Stem cells 2013;31:92–103.
[21] Prado-Lopez S, Conesa A, Arminan A, Martinez-Losa M, Escobedo-Lucea C, Gandia C, et al. Hypoxia promotes efficient differentiation of human embryonic stem cells to functional endothelium. Stem Cells 2010;28:407–18.
[22] Kusuma S, Peijnenburg E, Patel P, Gerecht S. Low oxygen tension enhances endothelial fate of human pluripotent stem cells. Arterioscler Thromb Vasc Biol 2014;34:913–20.
[23] Huang da W, Sherman BT, Lempicki RA. Systematic and integrative analysis of large gene lists using DAVID bioinformatics resources. Nat Protoc 2009;4:44–57.
[24] Huang da W, Sherman BT, Lempicki RA. Bioinformatics enrichment tools: paths toward the comprehensive functional analysis of large gene lists. Nucleic Acids Res 2009;37:1–13.
[25] Ohta R, Niwa A, Taniguchi Y, Suzuki NM, Toga J, Yagi E, et al. Laminin-guided highly efficient endothelial commitment from human pluripotent stem cells. Sci Rep 2016;6:35680.
[26] Hudon V, Berthod F, Black AF, Damour O, Germain L, Auger FA. A tissue-engineered endothelialized dermis to study the modulation of angiogenic and angiostatic molecules on capillary-like tube formation in vitro. Br J Dermatol 2003;148:1094–104.
[27] Newman AC, Nakatsu MN, Chou W, Gershon PD, Hughes CCW. The requirement for fibroblasts in angiogenesis: fibroblast-derived matrix proteins are essential for endothelial cell lumen formation. Mol Biol Cell 2011;22:3791–800.
[28] Sasagawa T, Shimizu T, Yamato M, Okano T. Expression profiles of angiogenesis-related proteins in prevascular three-dimensional tissues using cell-sheet engineering. Biomaterials 2014;35:206–13.
[29] Nolan DJ, Ginsberg M, Israely E, Palikuqi B, Poulos MG, James D, et al. Molecular signatures of tissue-specific microvascular endothelial cell heterogeneity in organ maintenance and regeneration. Dev Cell 2013;26:204–19.
[30] Minami H, Tashiro K, Okada A, Hirata N, Yamaguchi T, Takayama K, et al. Generation of brain microvascular endothelial-like cells from human induced pluripotent stem cells by co-culture with C6 glioma cells. PLoS One 2015;10:e0128890.